Electronic Supplementary Material (ESI) for Nanoscale.
This journal is © The Royal Society of Chemistry 2023

Supplementary information for "Thermal dynamics of few-layer-graphene seals"

Hjalte R. Ambjørner[1], Anton S. Bjørnlund[1], Tobias G. Bonczyk[2], Edwin Dollekamp[2], Lau M. Kaas[1], Sofie Colding-Fagerholt[1], Kristian S. Mølhave[3], Christian D. Damsgaard[1,2,3], Stig Helveg[1], Peter C. K. Vesborg[1,2]*

[1]Center for Visualizing Catalytic Processes (VISION), Department of Physics, Technical University of Denmark, DK-2800 Kgs. Lyngby, Denmark

[2]Surface Physics and Catalysis (SURFCAT), Department of Physics, Technical University of Denmark, DK-2800 Kgs. Lyngby, Denmark

[3]National Centre for Nano Fabrication and Characterization (Nanolab), Technical University of Denmark, DK-2800 Kgs. Lyngby, Denmark

*E-mail: peter.vesborg@fysik.dtu.dk

A. Cross section of cavities and the thickness of the electron-transparent cavity bottoms

The fabrication process defining the cavities of our device creates an undercut, and as a result, a cross section of a cavity is needed to determine the volume of the cavities. Using a Focussed Ion Beam (FIB) to cut through a cavity, SEM images of a cavity cross section could be obtained, see Fig. S1(a) and Fig. S1(b) for a cross section with and without sample tilt. The cavities are etched through a layer of SiO_2, and an isotropic etch is used to release the thin electron-transparent cavity bottoms from the silicon layer situated between the front surface and the SiO_2 layer defining the cavity bottoms. In Fig. S1, the electron-transparent bottom appears to be somewhat folded at the center of the cross section due to the cutting procedure. From the images presented in Fig. S1, the diameter of the cavities is estimated to be 6 μm.

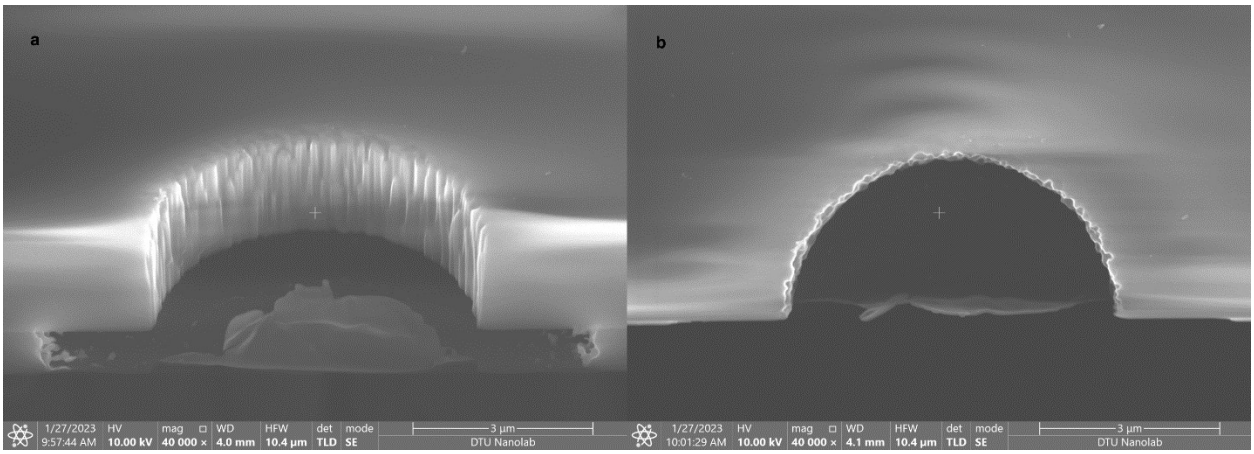

Fig. S1. A cross section of a cavity. a) *SEM micrograph of the cross section of a cavity obtained with the sample tilted* ***b)*** *SEM micrograph of the cavity acquired at zero tilt showing that the cross section passes through the center of the cavity.*

In order to estimate the thickness of the electron-transparent SiO_2 cavity bottoms, Energy-Filtered-Transmission-Electron-Microscopy (EFTEM) was performed. 9 cavities (three on each sample) were imaged with and without a 20 eV wide energy-selecting slit allowing only the elastically scattered electrons to contribute to the image. All images were acquired without an objective aperture. From each pair of images, a thickness-map can be generated, [1] and the resulting maps are presented in Fig. S2 with the thickness measured in terms of the mean free path, λ, of the beam electrons. The average thickness of the cavity bottoms is $\frac{t}{\lambda} = 0.27$ +/- 0.02 which corresponds to a SiO_2 thickness of 67 nm +/- 5 nm. [2]

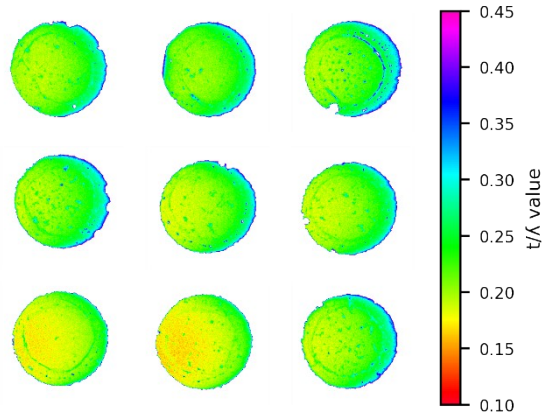

Fig. S2 Thickness maps of cavity bottoms. *The thickness is measured in terms of the mean free path, λ, of the beam electrons. The areas that stand out by their greater thickness are areas with silicon-residues left by the etch releasing the cavity bottoms.*

B. Optical images of samples

The few-layer-graphene-sealed (FLG-sealed) cavities investigated during this study are situated on three different samples. Optical images of the samples are shown in Fig. S3, and here, the electron-transparent cavities of the samples are clearly visible as black circular areas. As described in the main article, the cavities are etched into freestanding slabs, which in Fig. S3 appear gray. The cavities are arranged in a finder-grid, and each slab is marked with an electron-transparent number. Due to their absorption of light, the FLG-seals are gray in the optical images.

Apparent activation energies was determined for cavities denoted by letters in Fig. S3, and these energies are summarized in Table S1. Note that the investigated FLG-seal on sample 2 was damaged in the area with the cavities "f" and "g" during the experiments. Although, the distance to the edge of the FLG-seal varies, cavity a and c display similar apparent activation energies in temperature ramp 4. In addition, the distance from cavity b to the flake edge is similar to that of cavity a, however , the apparent activation energies for cavity b is different from that of cavity a in all cases. This strongly indicates that the apparent activation energy does not depend on the distance to the edge of the seal.

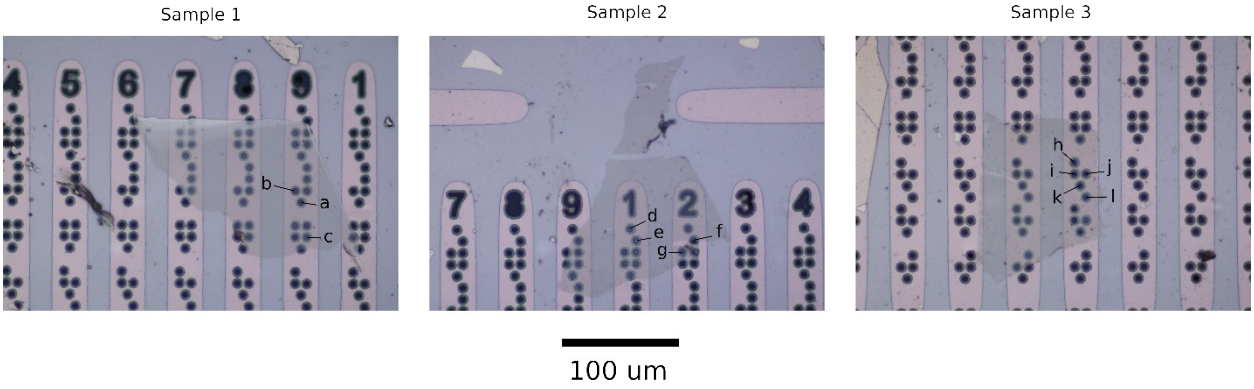

Fig. S3. Optical microscopy images of the three samples examined during this study. *Electron-transparent cavities (black) are organized in a finder-grid on freestanding slabs (grey) distinguishable by electron-transparent numbers. The FLG-seals appear gray on the blue background of the SiO_2 substrate.*

Sample 1			Sample 2			Sample 3		
Cav.	Ramp #	Ea	Cav.	Ramp #	Ea	Cav.	Ramp #	Ea
a	1	0.285±0.001	d	6	0.364±0.003	h	1	0.561±0.002
a	2	0.482±0.001	e	6	0.349±0.003	i	1	0.578±0.004
a	4	0.676±0.011	f	5	0.509±0.005	j	1	0.596±0.002
b	1	0.309±0.001	g	5	0.489±0.003	k	1	0.604±0.004
b	2	0.567±0.001				l	1	0.622±0.004
b	4	0.615±0.011						
c	4	0.68±0.006						

Table S1. Apparent activation energies determined from exponential fits to k-values (R^2 values greater than 0.99). *On Fig. S3 the position of the cavities "a"-"l" are indicated.*

C. Beam effects are negligible

If electron beam exposure affects the leak rate of argon, either at the start of or continuously during EELS acquisition, then, the decrease in argon content as a function of time will depend on how often measurements are conducted. In Fig. S4, the decay in argon signal retains its shape independent of the duration between EELS acquisitions, underlining that the leakage is not systematically induced or influenced by the beam. If the graphene-based-seal's impermeability is compromised by the electron beam, the leakage of argon will abruptly change. However, as mentioned in the main text, only exponential fits to the decreasing argon signal with *p*-values larger than 0.95 in a Pearson $\chi 2$-test are considered. As a result, leak rate measurements with abrupt changes in behavior are discarded. In general, the studied cavities display improved leak rates. Beam-induced phenomena are not likely to cause such behavior, and thus, in conclusion, beam-induced phenomena have negligible effect on our study.

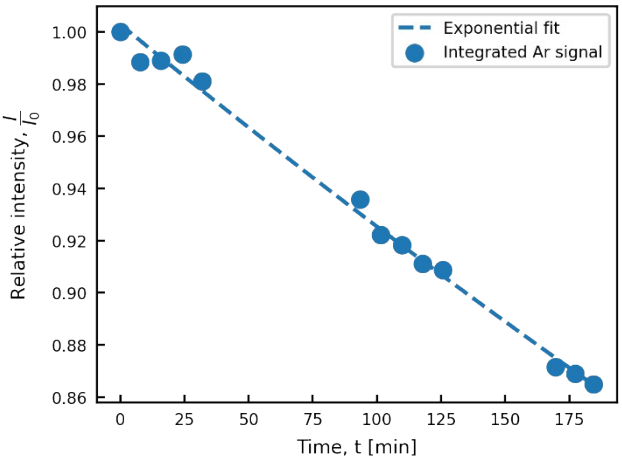

Fig. S4. Decrease in background-subtracted and integrated argon signal as a function of time. *Between the series of measurement points, the sample was left unexposed to the electron beam in the microscope vacuum. Since the total change in argon signal is small, the exponential fit (stippled line) cannot be distinguished from a linear fit, however, it is clear that the leak of argon from the investigated cavity is independent of the execution of EELS.*

D. The effect of a bulging seal

The graphene-based-seals bulge outwards when sealed cavities containing argon are exposed to the vacuum of the TEM. As a result, the total projected number of argon atoms is higher at the center of the cavities than at the edges. The greater the argon pressure is, the greater the effect will be. Potentially, this could cause the argon signal to scale non-linearly with argon pressure. To investigate the significance of this effect, two different areas of electron-beam illumination were used to acquire argon signal from five cavities. The illumination area utilized in the study of the leak rates was compared to a condition in which the whole of the cavity was illuminated. Note that the argon signal acquired with the wide illumination area does not vary with the bulging of the seal, as the electron current is equally distributed across the whole cavity, and so, both areas with high and low projected number of argon atoms are illuminated. In Fig. S5, the relative change in argon signal between the two conditions can be seen. As expected, the argon signal is largest when the smallest illuminated area near the center is used, but more importantly the difference between the two situations and between different measurements is only a few percent, comparable to the general uncertainty of our EELS methodology. The argon signals in this experiment are comparable in size to the largest argon signals observed in this study. Therefore, it is concluded that even in the case where the argon pressure is high, the shape of the seal does not have a large impact on the argon signal.

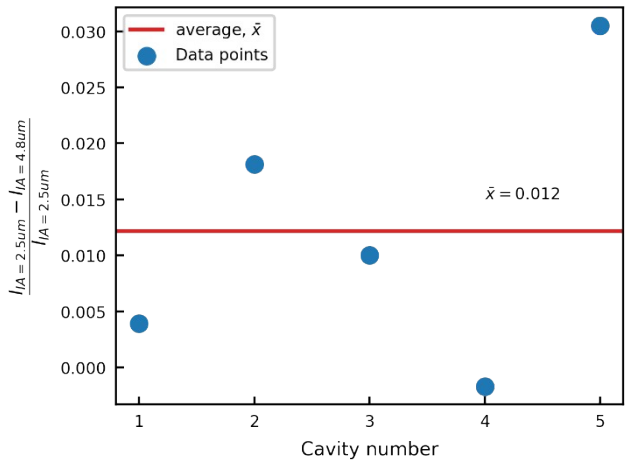

Fig. S5. Relative change in argon signal when changing between narrow and broad electron beam illumination.

E. P-values of a Pearson's chi-squared test

The temperature ramps were conducted such that appreciable changes in argon signal were observed within the timeframe of a TEM/EELS experiment, and the EELS acquisition procedure was optimized to produce relatively small uncertainty. Consequently, the exponential fits to the measured argon signal are in general

associated with quite large *p*-values in a Pearson's chi-squared test, as illustrated in Fig. S6(a). A few exponential fits perform much worse than others, however only 15/183 fits are associated with *p*-values lower than 0.95. Exponentials fits with associated *p*-values below 0.95 are not considered in the analysis of *k*-values. To illustrate that this is a reasonable cut-off, a box-plot of all obtained *p*-values is included in Fig. S6(a). The median of the *p*-values is shown with a line, and the box indicates the upper and lower quartiles. To represent the spread in the *p*-values, whiskers are plotted to mark the last *p*-value lying less than 1.5 times the interquartile range away from the upper and lower quartile. In the box-plot, *p*-values beyond the whiskers are plotted as individual black points. It is evident from a comparison between the box-plot and the scatter-plot of individual *p*-values that *p*-values below 0.95 are outliers.

The procedure of fitting the decreasing argon signal with an exponential function implicitly assumes that the leak can be described by a single exponential. This might not always be true. Throughout our study, we observed that heating can induce a change in leakage behavior. Potentially, such a change during a measurement of the leakage at a certain temperature could cause the leakage to deviate from a simple exponential behavior, see example on Fig. S6(b). Unless the FLG-seal is completely pierced, electron beam induced damage of the seal would be very difficult to distinguish from thermally induced phenomena. Hence, it cannot be excluded that beam damage can increase leak rates. Besides statistical fluctuations, we expect thermally induced-changes or beam induced-phenomena to be the reason why some of the exponential fits perform much worse than others in the Pearson's chi-squared test.

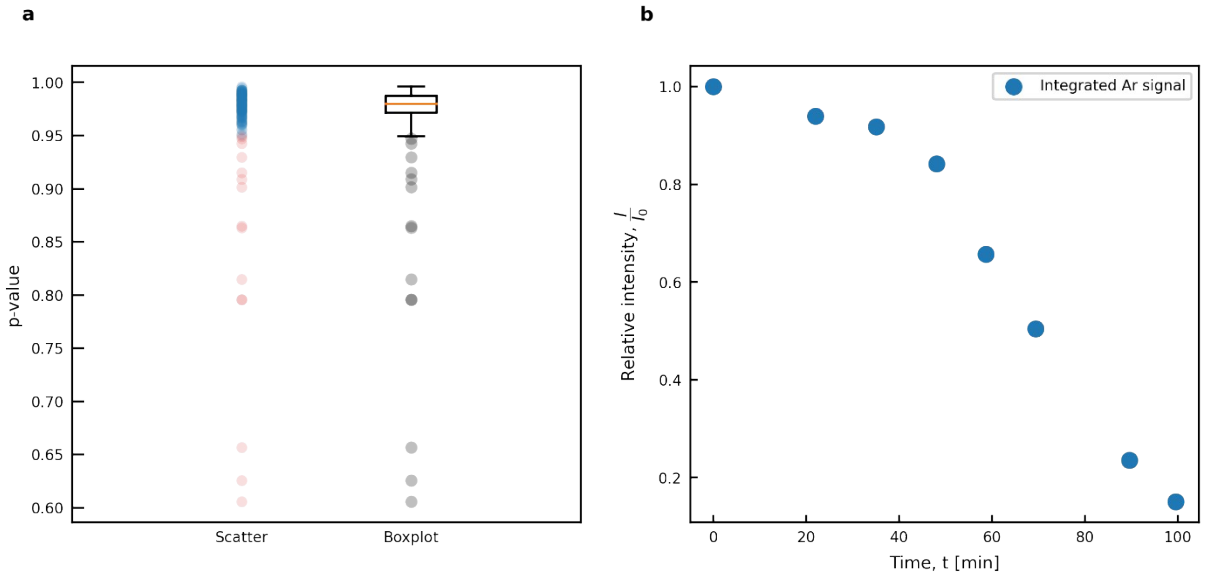

Fig. S6. a) *P-values obtained from a Pearson's chi-squared test of all the exponential fits for which (1) the k is greater than its uncertainty, (2) the fitted exponential decrease is above the sensitivity of our*

EELS methodology, and (3) the fit is based on at least 5 EELS measurements. Both a scatter plot of the individual p-values and a box-plot are shown. The box-plot indicates median, quantiles, and outliers. Only exponential fits with associated p-values above 0.95 (blue) are considered for further analysis. ***b)*** *Example of a change in leakage behavior at constant temperature.*

F. Changes in the *k*-values' temperature dependency

Due to the large number of observations of Arrhenius-like temperature dependencies, it was concluded in the main text that the *k*-values in general display Arrhenius-behavior. Sometimes, however, the *k*-values deviate from this temperature response, as seen in Fig. S7. We attribute these incidents to changes/jumps in leak-rate caused by a re-arrangement of the graphene-SiO_2 surface interface during a temperature ramp rather than an example of non-Arrhenius-like behavior. In Fig. S7(a), the *k*-value decreases during the third temperature ramp, when the temperature of the sample is increased from 300°C to 400°C. This behavior is incompatible with any regular diffusion, as diffusion fundamentally is a random walk with molecular/atomic motion caused by thermal energy, so higher temperatures should be associated with faster leakage. Based on this observation, it seems logical to conclude that the overall sealing, and thus the *k*-values, improved *during* the third temperature ramp. As mentioned in the main text, the samples were filled with argon at elevated temperatures between TEM temperature ramps, just as they are emptied of argon at elevated temperature. Since the gas-loading conditions experienced by the samples between measurements are similar to those experienced during temperature ramps, leak rates are likely to improve both during and between temperature ramps. Fig. S7(b) displays *k*-values from a cavity, which changes leak tightness more frequently during temperature ramps. Between the fourth and sixth temperature ramp, there is an atypical significant decrease in leak tightness. However, in the seventh temperature ramp, the sample achieved its most leak tight state. As written in the main text, our hypothesized mechanism driving the general improvement of the leak rates is not contradicted by cases of deteriorated leak tightness. *k*-values of both cavities presented in Fig. S7 display Arrhenius-like behavior and generally improved leak rates. Note, that the two cavities represented by the data in Fig. S7 exemplify the cases in which there is minimal and maximal deviation from the observed overall trend of an Arrhenius-type temperature dependency and improved leak-tightness as a result of heating.

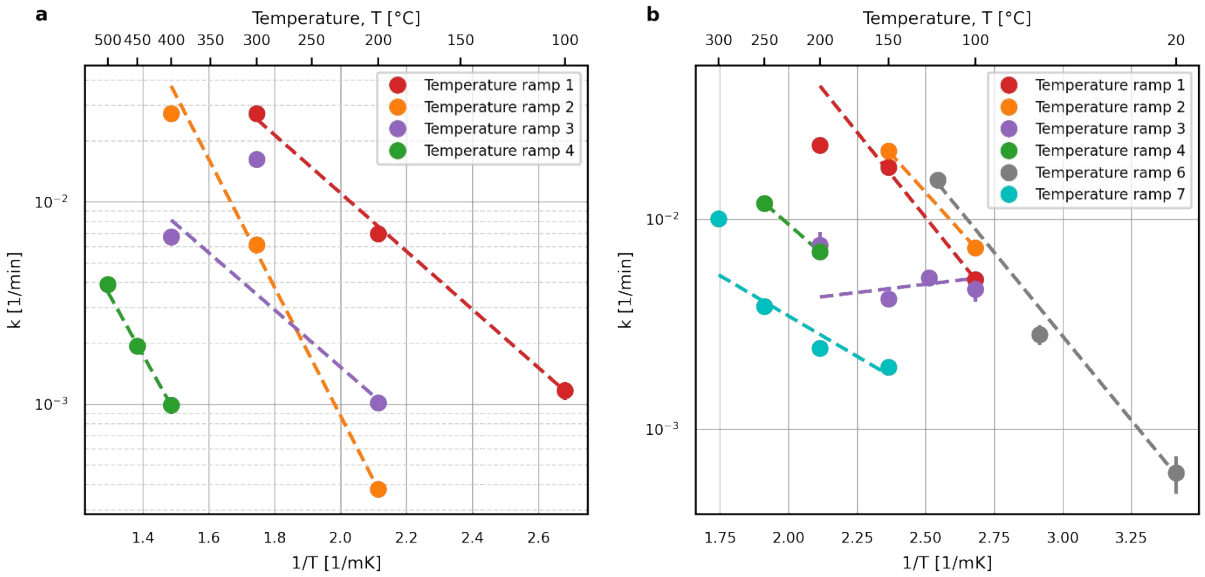

Fig. S7. Deviations from perfect Arrhenius behavior. *Scatter plot of k-values obtained on two different cavities,* ***a)*** *and* ***b)****, during multiple temperature ramps. Dots represent individual k-values and stippled lines indicate the best Arrhenius-like fits to the k-values.*

G. Calculation of leak rate at room temperature

The leak rate at room temperature, $\frac{\Delta N}{\Delta t}$, was estimated using the following equation:

$$\frac{\Delta N}{\Delta t} = N_{cav,rt} k_{rt}$$

$$k_{rt} = Be^{\frac{-E_a}{k_B T}}$$

$$N_{cav,rt} = C_{Ar} V_{cav} N_A$$

, where $N_{cav,rt}$ is the number of argon atoms in the cavity at room temperature calculated using molecular density in mole/volume, C_{Ar}, the volume of the cavity, V_{cav}, and Avogadro's number, N_A. The room temperature k-value, k_{rt} is estimated using E_a and B, which are extracted from an exponential fit to k's temperature dependency.

H. Generalization of improved leak rates resulting from thermal treatment

As stated in the main text, the k-values, in general, improved (i.e. decreased) drastically during our study. Data illustrating this phenomenon for one sample was presented in the main article (Fig. 4), and in Fig. S8, data from the remaining two samples are presented. Three temperature ramps were conducted on the sample

represented by Fig. S8(a), whereas 7 and 4 temperature ramps were conducted on the samples represented by Fig. S8(b) and Fig. 4(b), respectively.

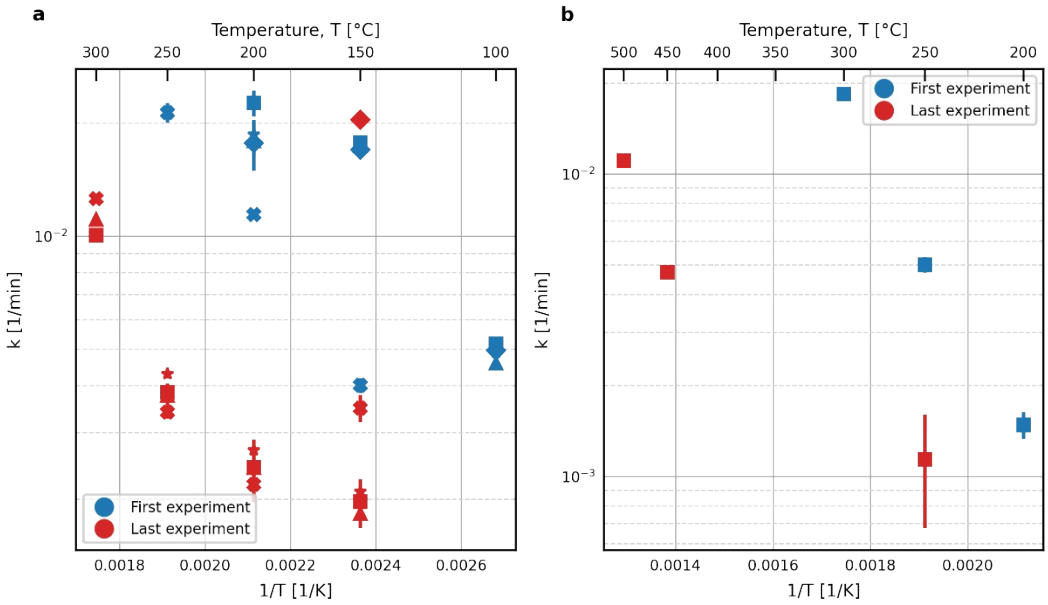

Fig. S8. *k-values obtained on the same cavities during the first and last temperature ramp conducted on two of the three investigated samples. Squares, triangles, and stars are used to indicate different cavities.*

I. Sensitivity of EELS procedure

The uncertainty of our EELS methodology can be estimated from repeated measurements of an argon signal, which, in principle, should be constant. Five cavities were used for such a test. The cavities were filled with argon and the background-subtracted and integrated argon signal was monitored at ambient temperature. The relative change in argon signal as compared to the first measurement of argon content obtained on the respective cavities is presented in Fig. S9. It is obvious from the figure that in this experiment, the leakage cannot be resolved, and hence variations in the data can be used to estimate the inherent uncertainty of our measurements. Assuming random noise, the true argon signal lies with 95% certainty within two standard variations of the measured signal. To unambiguously distinguish measured signals, we define our sensitivity as four times the standard deviation determined from Fig. S9. Furthermore, we only consider background-subtracted and integrated argon signals more than two standard deviations above zero. Note that fluctuations in argon signal associated with moving between cavities are, if present, included in the uncertainty defined this way.

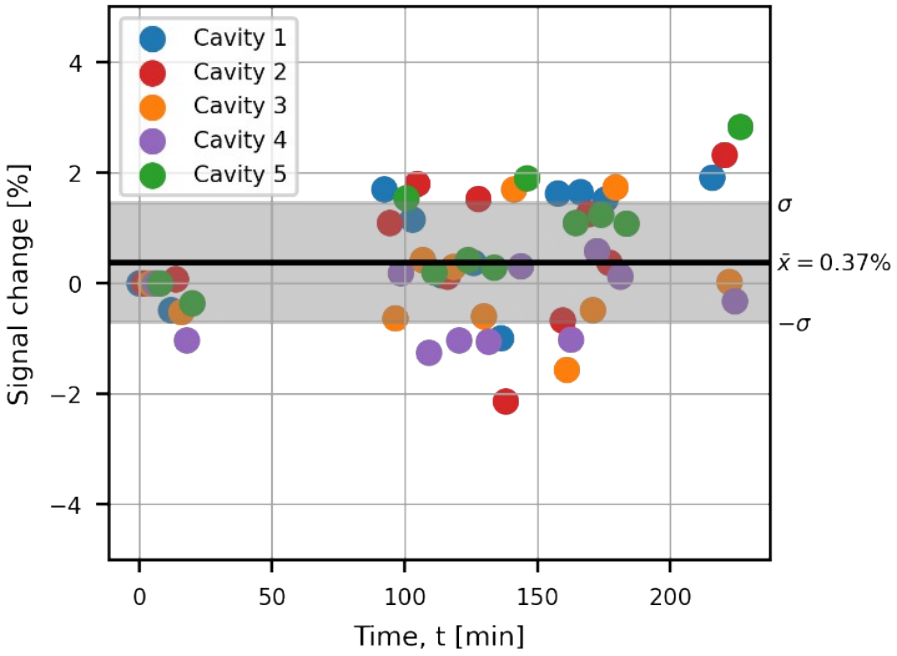

Fig. S9. Sensitivity of our methodology. *Measurements of the argon content of 5 different cavities with no leak during the experiment. The argon signal obtained on each cavity is plotted in terms of the relative change to the first argon signal acquired on the respective cavities.*

References

1 R. F. Egerton, *Electron energy-loss spectroscopy in the electron microscope*, Springer, 2011.

2 C. W. Lee, Y. Ikematsu and D. Shindo, *J Electron Microsc (Tokyo)*, 2002, **51**, 143–148.